Protonic Diffusion in High-Pressure Ice VII

Eriko Katoh, H. Yamawaki, H. Fujihisa, M. Sakashita, K. Aoki*

Near ambient pressures, molecular diffusion dominates protonic diffusion in ice. Theoretical studies have predicted that protonic diffusion will dominate at high pressures in ice. We measured the protonic diffusion coefficient for the highest temperature molecular phase of ice VII at 400 kelvin over its entire stable pressure region. The values ranged from 10^{-17} to 10^{-15} square meters per second at pressures of 10 to 63 gigapascals. The diffusion coefficients extrapolated to high temperatures close to the ice VII melting curve were less by a factor of 10^2 to 10^3 than a superionic criterion of $\sim 10^{-8}$ square meters per second, at which protons would diffuse freely.

Protons can move in the hydrogen-bonded network of water molecules by transferring within a hydrogen bond and then jumping into another hydrogen bond by molecular rotation. Although this diffusion model specific to ice was proposed in the middle of the 20th century (*1*), its process has eluded experimental investigation. The protonic diffusion coefficient estimated for ambient-pressure ice at 263 K is on the order of 10^{-20} m^2/s, which is four to five orders of magnitude less than the molecular diffusion coefficient (*2–4*). The fast molecular diffusion interferes with observation of the slow protonic diffusion. Dielectric properties and electrical conductivity, which can be related to protonic diffusion coefficients, have been measured for pure and doped ices instead (*5–9*).

Theoretical studies have consistently predicted the presence of a superionic (or superprotonic) phase characterized by a fast protonic diffusion with a coefficient of $\sim 10^{-8}$ m^2/s at extremely high temperatures and pressures (*10*, *11*). The superionic state is predicted to appear in the phase diagram at about 1000 K and 20 GPa and to develop to higher temperatures ranging from 2000 to 4000 K above 100 GPa. In the superionic phase, the protons are thought to move quickly by jumping successively between their neighboring occupation sites in a crystal lattice consisting solely of oxygen atoms. Such a superionic phase can be characterized as a partially melted state and can be compared with ionic fluid or a fully melted state in which neutral or ionized water molecules diffuse freely. The superionic phase of ice may play a crucial role in the generation of the magnetic fields in giant planets as well as the metallic fluid of water (*11–14*).

Here, we report on protonic diffusion measurements carried out for ice VII over its entire stable pressure region from 2 to about 60 GPa (*15–19*). The mutual diffusion process of protons and deuterons was observed in an H_2O/D_2O ice bilayer pressurized in a high-pressure optical cell [a diamond anvil cell (DAC)] by measuring its time-dependent infrared reflection spectra. The diffusion coefficient was determined at pressures of 10.2, 14.1, 32.2, and 63 GPa at a fixed temperature of 400 K. The predicted temperature range of the superionic ice was located far above that accessible with the DAC technique. However, the obtained diffusion results allowed us to examine the phase diagram theoretically proposed for high-temperature and high-pressure ices, including those at the superionic phase.

We used an H_2O/D_2O ice bilayer assembly for measuring the protonic diffusion process at high temperature and pressure (Fig. 1A). Protonic diffusion from an H_2O layer of thickness l_H to a D_2O layer of thickness l_D is described in a one-dimensional model by

$$C_H(x,t) = \frac{l_H}{l} + \sum_{n=1}^{\infty} \frac{2}{n\pi} \sin\left(\frac{n\pi l_H}{l}\right) \cos\left(\frac{n\pi x}{l}\right) \exp\left\{-\left(\frac{n\pi}{l}\right)^2 Dt\right\}$$

where $C_H(x, t)$ is the concentration of protons at location x and diffusion time t, l is the whole sample thickness equal to $l_H + l_D$, and D is the mutual diffusion coefficient (*20*). For the proton concentration at $x = l$, or the outer surface of the D_2O ice layer, the equation becomes simply a function of diffusion time t. The surface concentration $C_H(l, t)$ thus deduced will rise abruptly on the first arrival of diffused protons and will increase toward its steady value of l_H/l with the progression of diffusion. We can hence derive a diffusion coefficient, D, from time-dependent spectra measured for the outer surface of the D_2O ice layer. For the surface concentration of deuterons at the opposite side of the ice bilayer, an equivalent description $C_D(0, t)$ can be readily derived with the thickness of D_2O ice layer l_D.

We first examined a spectral measurement at the ambient temperature of 298 K and found no spectral change with time even 1 month after the sample preparation. We further examined spectral measurements at several higher tem-

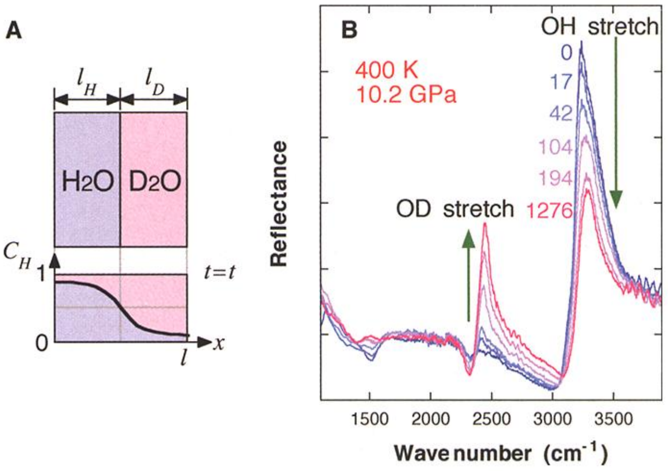

Fig. 1. An H_2O/D_2O ice bilayer assembly for protonic diffusion measurement (**A**) and the reflection spectra measured for the H_2O outer surface of the ice bilayer (**B**). An H_2O/D_2O ice bilayer sample was prepared in the sample chamber of a DAC, typically 100 μm in diameter and 40 μm in depth, by the following steps. The chamber was first filled with liquid D_2O (99.96% deuterated) and sealed with a small end plug 100 μm in diameter and 20 μm long, just half of the chamber depth. The DAC was cooled with liquid nitrogen to about 200 K to freeze the contained liquid. The end plug was removed, and deionized H_2O vapor was deposited into the empty top half of the chamber. The sample was quickly pressurized to approximately 10 GPa in the DAC to confine the H_2O/D_2O ice bilayer so that the sample was solid when warmed to ambient temperature. The thickness of the D_2O ice layer and of the H_2O/D_2O ice bilayer was determined by interferometric measurement (*28*) using the refractive index of high-pressure ice (*28*, *29*). The reflection spectra were measured for the sample annealed at 400 K and 10.2 GPa. The numbers attached to the spectra represent annealing (diffusion) time in hours. The spectra were corrected for the absorption and reflection from the DAC using a reference spectrum measured in advance with a KBr-filled DAC.

National Institute of Advanced Industrial Science and Technology, Tsukuba Central 5, Tsukuba 305–8565, Ibaraki, Japan.

*To whom correspondence should be addressed. E-mail: k-aoki@aist.go.jp

peratures and found that an annealing temperature of 400 K produced a protonic diffusion rate appropriate for the present spectroscopic measurement. The sample was annealed isothermally for several hours to several tens of hours in an electric oven and quenched to room temperature for spectral measurement. We repeated thermal annealing and spectral measurement several tens of times until the spectral change due to mutual diffusion was completed. Each run of the diffusion experiment at a given pressure required a measuring time of 1000 hours or more.

Infrared reflection spectra measured for the H_2O outer surface of an H_2O (L_H = 14 μm) and D_2O (l_D = 16 μm) ice bilayer annealed at 400 K and 10.2 GPa are shown in Fig. 1B. The OD stretching peak located approximately at 2400 cm^{-1} gradually increased in height with time, whereas the OH stretching peak located approximately at 3200 cm^{-1} gradually decreased. These spectral changes are attributed to the mutual diffusion of protons and deuterons through the H_2O and D_2O layered interface, and those changes last until the isotopes diffuse homogeneously over the whole ice crystal.

Because molecular migration is dominant in the diffusion process of ambient-pressure ice (*2–4*), we examined the possibility of molecular diffusion by measuring reflection spectra with an $H_2{}^{16}O/H_2{}^{18}O$ ice bilayer annealed at the same temperature and pressure (400 K and 10.2 GPa). The spectra measured for both outer surfaces of the ice bilayer differed by 16 cm^{-1} in the OH stretching peak position. The peak positions did not change, even after 600 hours, indicating no signal for the molecular diffusion. We melted the sample by releasing pressure slightly and then solidified it again by increasing pressure back to 10.2 GPa. The peak positions then moved to the middle point between the original ones, indicating mixing of the $H_2{}^{16}O$ and $H_2{}^{18}O$ molecules in the liquid phase. The possibility of molecular diffusion was hence ruled out for ice VII highly densified under pressure.

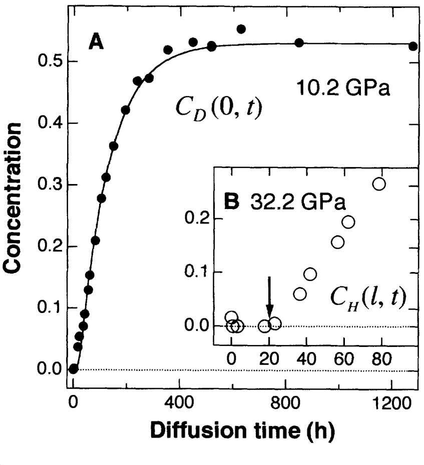

Fig. 2. Variation of the surface concentration of deuteron $C_D(0, t)$ with diffusion time measured for the H_2O outer surface of the ice bilayer (**A**). The sample was annealed at 400 K and 10.2 GPa. The inset shows the beginning of the variation of proton concentration $C_H(l, t)$ measured for the D_2O outer surface at 32.2 GPa (**B**).

The variation of the surface concentration of isotopes with diffusion time is shown in Fig. 2. The deuteron concentration $C_D(0, t)$ measured for the outer surface of the H_2O ice layer at 10.2 GPa (Fig. 2A) rises immediately and approaches a steady value of l_D/l = 0.53 with time. The profile of surface concentration versus diffusion time thus obtained was fitted by the diffusion equation derived for the surface concentration to yield a diffusion coefficient of $D = 2.3 \times 10^{-16}$ m^2/s. The variation of proton concentration [$C_H(l, t)$] measured for the outer surface of D_2O ice at a higher pressure of 32.2 GPa (Fig. 2B) shows an onset of rapid increase in concentration located at $t \sim 20$; the protons require at least 20 hours to pass through the 7.5-μm-thick D_2O ice layer. Such a delay of rising time was not clearly observed for the deuteronic diffusion at 10.2 GPa through a 14-μm-thick H_2O ice layer. The diffusion rate, which lessens noticeably with an increase in pressure to 32.2 GPa, was determined to be between 5.2×10^{-17} and 7.6×10^{-17} m^2/s by the accurate fitting procedure.

The diffusion coefficients measured at 400 K show a monotonic decrease by two orders of magnitude with increasing pressure up to 63 GPa (Fig. 3). The diffusion coefficient can be described by $D = D_0\exp(-\gamma P/kT)$, where γ represents the magnitude of pressure influence on the activation energy for the protonic diffusion motion. Fitting the obtained diffusion coefficients by this exponential expression provided 0.003 eV/GPa for γ. Although no experimental data are available for the activation energy at ambient pressure, ΔE_0, we may assume it to be equal to that determined from the electric conductivity measurement on pure ice at ambient pressure (*9*). The activation energy, $\Delta E = \Delta E_0 + \gamma P$, is thus rewritten as $\Delta E = 0.70 + 0.003P$, where ΔE and ΔE_0 are presented in eV and P in GPa.

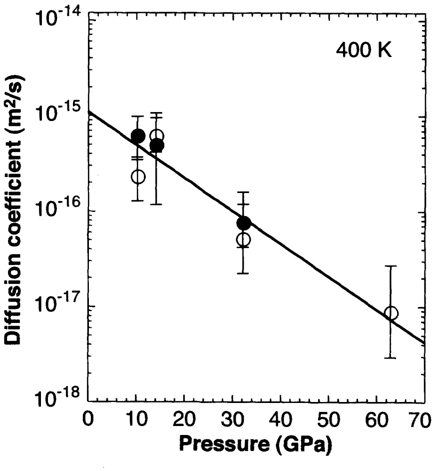

Fig. 3. Variation of the protonic diffusion coefficient with pressure measured for ice VII. Open and solid circles represent those obtained from reflection spectra measured for the H_2O and D_2O outer surfaces of the H_2O/D_2O bilayer, respectively.

The variation of diffusion coefficient with pressure appears to be contrary to that expected from the distinct change in the hydrogen bonding state associated with the molecular to nonmolecular transition in ice VII. In the molecular state at low pressures, the protonic diffusion proceeds by two steps: transfer in a hydrogen bond and then a jump into another hydrogen bond. For ambient-pressure ice, the activation energies were experimentally determined by infrared absorption measurement to be 0.41 eV for the transfer and 0.52 eV for the jump (*21*). In the nonmolecular region around 60 GPa, the energy barrier for the transfer motion vanishes and allows the protons to transfer freely along the hydrogen bonds to form ionized molecular species (*22–26*). The diffusion process can be described as a single step involving a proton jump alone, and we expected the process to be accelerated by increases in the population of ionized molecular species. Nevertheless, the diffusion coefficient decreased in this pressure region. The diffusion process would alter gradually from the two-step process to a single-step process, while ice VII also transformed gradually from the molecular to the nonmolecular state.

On the basis of our experimental data at 400 K and our value for ΔE, we calculated that the diffusion coefficient would increase to $\sim 10^{-11}$ m^2/s at 20 GPa in the molecular state and to $\sim 10^{-10}$ m^2/s at 60 GPa in the nonmolecular state. These values are less by a factor of 10^2 to 10^3 than the superionic criterion of $\sim 10^{-8}$ m^2/s. A fast protonic diffusion state would not be realized in the ice VII region, but in the superionic phase would be predicted to appear as an intermediate phase between ice VII and fluid.

References and Notes

1. N. Bjerrum, *Science* **115**, 385 (1952).
2. H. Blicks, O. Dengel, N. Riehl, *Phys. Kondens. Mater.* **4**, 375 (1966).
3. R. O. Ramseier, *J. Appl. Phys.* **38**, 2553 (1967).
4. K. Itagaki, *J. Phys. Soc. Jpn.* **22**, 427 (1967).
5. G. C. Camplin, J. W. Glen, J. G. Paren, *J. Glaciol.* **21**, 123 (1978).
6. M. Hubmann, *J. Glaciol.* **21**, 161 (1978).
7. I. Takei, N. Maeno, *J. Phys.* **48** (*Colloque C1*), 121 (1987).
8. S. Kawada, R. G. Jin, M. Abo, *J. Phys. Chem. B* **101**, 6223 (1997).
9. V. F. Petrenko, R. W. Whitworth, *J. Phys. Chem.* **87**, 4022 (1983).

→ P. Demontis, R. LeSar, M. L. Klein, *Phys. Rev. Lett.* **60**, 2284 (1988).

11. C. Cavazzoni *et al.*, *Science* **283**, 44 (1999).

→ D. J. Stevenson, *Rep. Prog. Phys.* **46**, 555 (1983).

13. W. J. Nellis *et al.*, *Science* **240**, 779 (1988).
→ W. J. Nellis *et al.*, *J. Chem. Phys.* **107**, 9096 (1997).
15. W. F. Kuhs, J. L. Finney, C. Vettier, D. V. Bliss, *J. Chem. Phys.* **81**, 3612 (1984).
→ R. J. Hemley *et al.*, *Nature* **330**, 737 (1987).
17. M. Song *et al.*, *Phys. Rev. B* **60**, 12644 (1999).
18. Ph. Pruzan *et al.*, *J. Phys. Chem. B* **101**, 6230 (1997).
19. A. F. Goncharov *et al.*, *Phys. Rev. Lett.* **83**, 1998 (1999).
20. J. Crank, *The Mathematics of Diffusion* (Clarendon, Oxford, 1975), pp. 44–68.
21. W. B. Collier, G. Ritzhaupt, J. P. Devlin, *J. Phys. Chem.* **88**, 363 (1984).
22. K. S. Schweizer, F. H. Stillinger, *J. Chem. Phys.* **80**, 1230 (1984).
23. P. G. Johannsen, *J. Phys. Condens. Matter* **10**, 2241 (1998).
→ M. Benoit, D. Marx, M. Parrinello, *Nature* **392**, 258 (1998).
25. ———, *Solid State Ionics* **125**, 23 (1999).
26. W. B. Holzapfel, *Physica B* **265**, 113 (1999).
27. R. Le Toullec, P. Loubeyre, J. P. Pinceaux, *Phys. Rev. B* **40**, 2368 (1989).
28. H. Shimizu, T. Nabetani, T. Nishiba, S. Sasaki, *Phys. Rev. B* **53**, 6107 (1996).
29. The experimental data available were limited to 8 GPa. We estimated the high-pressure values using an experimentally obtained refractive index vs. pressure relation and the Lorentz-Lorenz equation $(n^2 - 1)/(n^2 + 2) = (4/3)\pi\alpha N_A/V$, where n, α, N_A, and V are refractive index, polarizability (assumed to be constant), Avogadro's number, and molar volume, respectively.
30. We thank K. Terakura and T. Ikeda for discussion on the protonic diffusion mechanism in high-pressure ice.

5 November 2001; accepted 7 January 2002

Chiral Amplification of Oligopeptides in Two-Dimensional Crystalline Self-Assemblies on Water

Helmut Zepik,[1] Edna Shavit,[1] Mao Tang,[1] Torben R. Jensen,[2]
Kristian Kjaer,[2] Gérard Bolbach,[3] Leslie Leiserowitz,[1]*
Isabelle Weissbuch,[1]* Meir Lahav[1]*

Differences in the two-dimensional packing arrangements of racemic and enantiomeric crystalline self-assemblies on the water surface of amphiphilic activated analogs of lysine and glutamic acid have been used to prepare oligopeptides of homochiral sequence and oligopeptides of single handedness from chiral nonracemic mixtures. The crystalline structures on the water surface were determined by grazing incidence x-ray diffraction and the diastereomeric composition of the oligopeptides by matrix-assisted laser desorption time-of-flight mass spectrometry with enantio-labeling. These results suggest that reactivity of ordered clusters at interfaces might have played a role in the generation of early homochiral biopolymers.

Theories on the emergence of the homochiral biopolymers of life at prebiotic times suggest the involvement of enantioselective reactions starting from heterochiral mixtures of α–amino acid and nucleic acid precursors (*1–7*). Polymerization reactions of racemates in isotropic media would lead, however, to formation of polymers comprising a random sequence of left (*S*)- and right (*R*)-handed repeat units in a binomial distribution (*8*). Thus, the probability of obtaining oligomers with homochiral sequence will become negligible with increasing length (*9–11*). A possible way to obtain oligopeptides of homochiral sequence from racemic mixtures would be through the self-assembly of the precursor molecules into ordered architectures followed by lattice-controlled reactions.

Two-dimensional (2D) self-assemblies formed at the water surface provide an ideal medium for the performance of stereospecific and enantioselective chemical reactions because (i) they promote effective molecular ordering, (ii) they permit substantial molecular flexibility, and (iii) they allow access to the ordered, flexible molecules by other reagents from the aqueous subphase (*12–14*). Moreover, with the recent advent of grazing incidence x-ray diffraction (GIXD) using synchrotron radiation, it became possible to determine the structure of the crystalline components of these assemblies at the molecular level, providing an important tool for the design of new architectures and control of their reactivity (*15*).

Racemic mixtures of amphiphilic molecules at interfaces can self-assemble into 2D crystallites of three types: (i) racemic compounds in which both enantiomers are packed together, (ii) enantiomorphous conglomerates involving segregation of the enantiomers (*16*), and (iii) enantiomerically disordered solid solutions. Here, we focus on activated α–amino acid derivatives that self-assemble into 2D crystallites as racemic compounds that, upon polymerization, yield oligopeptides with an enhanced homochiral (isotactic) sequence, as shown, in principle, in Scheme 1A. This concept is illustrated with the polycondensation of racemic N^{ε}-stearoyl-lysine-thioethylester (C_{18}-TE-Lys).

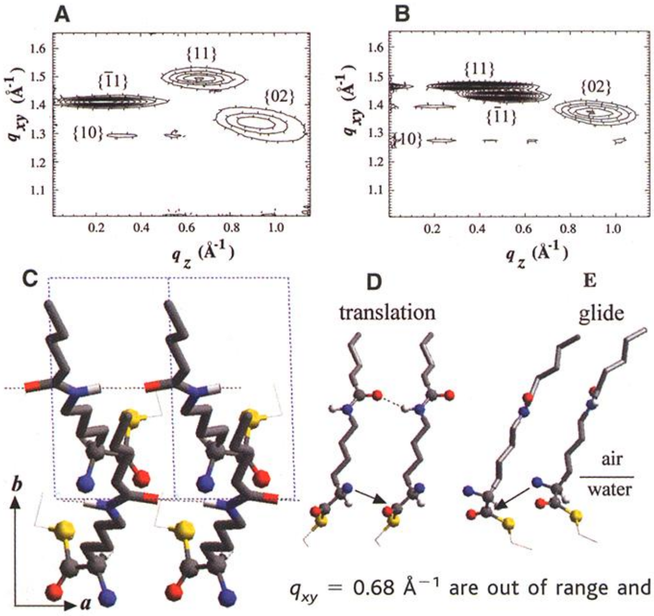

Fig. 1. GIXD patterns $I(q_{xy}, q_z)$ of the self-assembled 2D crystallites of C_{18}-TE-Lys on water at 4°C, where q_{xy} and q_z are horizontal and vertical components of the x-ray scattering vector. **(A)** Enantiomerically pure. **(B)** Racemate. **(C)** The packing arrangement of the racemic compound viewed perpendicular to the water surface. **(D and E)** Pairs of molecules related by translation and by glide symmetry, respectively, viewed parallel to the water surface. For clarity, part of the hydrocarbon chains is not shown. In (A) and (B) the {01} Bragg peaks at q_{xy} = 0.68 Å^{-1} are out of range and are not shown for clarity.

---

[1] Department of Materials and Interfaces, Weizmann Institute of Science, 76100 Rehovot, Israel. [2] Materials Research Department, Risø National Laboratory, 4000 Roskilde, Denmark. [3] Laboratoire de Chimie Structurale Organique et Biologique, Université Pierre et Marie Curie, 75252 Paris Cedex 05, France.

*To whom correspondence should be addressed. E-mail: leslie.leiserowitz@weizmann.ac.il, isabelle.weissbuch@weizmann.ac.il, meir.lahav@weizmann.ac.il